General and Comparative Endocrinology 284 (2019) 113268

Contents lists available at ScienceDirect

General and Comparative Endocrinology

journal homepage: www.elsevier.com/locate/ygcen

Reversal of ciprofloxacin-induced testosterone reduction by probiotic microbes in mouse testes

Congcong Xie[c,1], Yanqing Bian[d,1], Helin Feng[e,1], Yu Zhao[a], Lixuan Wang[a], Yaru Li[f], Dong Zhang[d], Yangyang Tian[a], Li Li[a], ShiYang Chang[a], Hang Li[a], Xiujun Zhao[a,*], Pin Lv[b]

[a] Department of Histology and Embryology, Hebei Medical University, Shijiazhuang 050017, China
[b] Institute of Chinese Integrative Medicine, Hebei Medical University, Shijiazhuang 050017, China
[c] Research Institute of Family Planning of Hebei Province, Key Laboratory for Family Planning and Birth Health of the National Health and Family Planning Committee, Shijiazhuang 050071, China
[d] College of Life Science, Hebei Normal University, Shijiazhuang 050024, China
[e] The Fourth Hospital of Hebei Medical University, Shijiazhuang 050011, China
[f] Institute of Chemistry, Chinese Academy of Sciences, Beijing 100190, China

ARTICLE INFO

Keywords:
Ciprofloxacin
Bifidobacteria
Testosterone
NF-κB
Sirt1
Inflammatory cytokine

ABSTRACT

CPFX is a highly effective antibiotic, but it has been reported to significantly impair both testicular function and structure in rats. In this study, we assessed reversal of CPFX-induced variation in mice testicular structure and testosterone synthesis by probiotic microbes in the infected model and normal model. We detected testicular weight, testicular structure and Leydig cell variables in numbers. We detected the levels of serum testosterone and steroidogenic enzymes, as well as DBC1, Sirt1, NF-κB, and related redox state and inflammatory response in the testes. The results showed that probiotic microbes had significantly elevated serum testosterone levels and steroidogenic enzymes, higher Sirt1, anti-oxidative enzymes and anti-inflammatory cytokine expression, and lower NF-κB, DBC1, oxidative damage, pro-inflammatory cytokine expression. The results suggest that the testis-protective, antiinflammatory and antioxidation effects of probiotics largely resulted from its ability to decrease oxidative stress and preserve antioxidant activity by stabilizing antioxidant defense systems, reducing oxidative damage and inflammatory response.

1. Introduction

Ciprofloxacin (CPFX) is a member of a promising new class of antimicrobial agents known as fluoroquinolones, which are an important group of antibiotics routinely administered by urologists and fertility specialists in order to control infections in male reproductive organs (Ryan et al., 2018). However, various studies have reported that short-term administration of CPFX can promote toxicity in male reproductive tissues and remarkable degeneration of Leydig cells (Zobeiri et al., 2013).

While the mechanisms by which CPFX elicits the above effects are not well understood, they are likely mediated by oxidative stress, which is manifested by the production of excess reactive oxygen species (ROS) and lead to oxidative damage to DNA, proteins, and membrane lipids (Kalghatgi et al., 2013). The mechanisms may also involve changes in proinflammatory cytokines (Shaki et al., 2016). Some proinflammatory cytokines, such as tumor necrosis factor-α (TNF-α) and interleukin (IL)-1β, have been demonstrated to have inhibitory effects on the expression of steroidogenic enzymes and dramatically decrease serum testosterone levels (Leisegang and Henkel, 2018; Bornstein et al., 2004; Tremellen et al., 2018). Nuclear factor kappa beta (NF-κB) is a redox-sensitive transcription factor that is involved in the expression of genes encoding pro-inflammatory molecules (such as IL-1β) (Steiner et al., 2018). Silent Mating Type Information Regulation 2 Homolog 1 (Sirt1), a member of the silent information regulator family, has been suggested to play a vital role in protection against the proinflammatory response in Leydig cells by inhibiting the NF-kB signaling pathway (Iskender et al., 2018). Interestingly, the deleted in breast cancer 1 (DBC1) protein has been reported to be a key physiological regulator of Sirt1 activity (Nohr et al., 2017; Liu et al., 2016; Li et al., 2019). SIRT1, also a redox sensor,

---

[*] Corresponding authors at: Department of Histology and Embryology, Hebei Medical University, 361, zhongshan Eastern Road, Shijiazhuang, Hebei Province 050017, China (X. Zhao).
E-mail address: 284805563@qq.com (X. Zhao).
[1] These authors contributed equally to this study.

https://doi.org/10.1016/j.ygcen.2019.113268
Received 18 March 2019; Received in revised form 19 August 2019; Accepted 1 September 2019

has shown to protect neural cells from oxidative stress in part by repressing the expression of NF-κB (Singh et al., 2017). Considering the influence of Sirt1 on oxidative stress, NF-κB and inflammatory pathway, its expression in the testes in response to CPFX was also investigated in this study.

Probiotics are mono or mixed cultures of live microorganisms which if administered in adequate amounts can confer a health benefit to the host. Lactic acid bacteria (LAB) and bifidobacteria are the most common types of microbes used as probiotics (Bubnov et al., 2018). Some studies have found that the dietary supplementation of aged mice with probiotics results in a younger appearance, larger testes and more dominant male behavior compared with their matched untreated sibling mice (Poutahidis et al., 2014). Interestingly, these effects were linked with down-regulation of pro-inflammatory cytokines (Holowacz et al., 2018; Ermolenko et al., 2018). Karamali study also found that a serum inflammatory marker and C-reactive protein (CRP) were reduced with the consumption of probiotics (Karamali et al., 2018). Other researches have shown that the beneficial effects of the probiotics may be related to their ability to reduce oxidative stress (Wang et al., 2017). Bifidobacterium animalis 01 were found to scavenge ROS in vitro while enhancing the antioxidase activities of mice in vivo (Shen et al., 2011). Furthermore, the oxidative stress in patients with type 2 diabetes can be ameliorated by multispecies probiotics (Asemi et al., 2013). Therefore, in this study we tested the hypothesis that dietary probiotics may act to reverse CPFX-stimulated reduction in serum testosterone levels in the normal and infected models and that the beneficial effects of probiotic consumption may be conferred by inhibition of oxidative damage and inflammatory state.

2. Materials and methods

2.1. Preparation of bifidobacteria

Bifidobacteria strains were cultured in MRS media (pH 6.2) at 37 °C for 20 h under anaerobic conditions. The bifidobacteria formed detectable numbers of colonies (i.e., $\geq 10^8$ cfu/mL) in MRS media. Bacterial cultures were centrifuged at 8000 rpm for 10 min at 4 °C and washed with 0.9% saline solution twice. The concentration of bifidobacteria based on a previously published protocol (Savignac et al., 2015), and the dosage of bifidobacteria was determined with 10^9 cfu/mL/day. The collected bifidobacteria (1×10^9 cfu/ml) were suspended in 50 ml 0.9% saline solution and stored at 4 °C.

2.2. Animals and experimental design

Adult male Kunming mice (3–4 months old, 35–40 g in weight) purchased from the Laboratory Animal Center of Hebei Medical University were used for all of the experiments. Animals were maintained at standard temperature (22 ± 1 °C) and relative humidity (60%) conditions with a 12-h light–dark cycle and free access to food and water. They were allowed 5 days of habituation to the environment before use in experiments.

To assess the administering time of bifidobacteria, these animals in normal model and epididymitis-orchitis model treated with CPFX were administered with 1×10^9 cfu/ml bifidobacteria for the different time periods from 6 to 64 days as different groups: BI_6, BI_{18}, BI_{30}, BI_{42}, BI_{64} (BI means bifidobacteria). The administering times of bifidobacteria depended on testosterone level.

The fifty mice were randomly divided into 5 groups of 10 animals per group as a normal model: saline as vehicle for 6 days (Sal group); bifidobacteria (10^9/mL) in saline as vehicle for 6 days (BI group); 200 mg/kg/day of CPFX in saline as vehicle for 6 days (which represents the therapeutic dose of the drug in humans) (CP group); After CPFX for 6 days, then animals were administered bifidobacteria (10^9/mL) in saline. CPFX for 6 days then normal saline for 6 days (CP + Sal group); CPFX for 6 days and then bifidobacteria (10^9/mL) in saline as vehicle for 6 days (CP + BI group). Animals of each group were administered the vehicle by gavage in two equally divided doses per day.

Another forty mice (Prepare for the pre-experiment) were divided into four groups as a epididymitis-orchitis model: Control group (Con) did not undergo any intervention. Epididymo-orchitis group (EO) was induced by injecting 50ul Escherichia coli suspension (10^6 cfu/mL, ATCC 25922) into the epididymal direction of the proximal right vas deferens as described previously (Ludwig et al., 2002). 200 mg/kg/day of CPFX in saline as vehicle for 6 days. After CPFX for 6 days, then animals were administered bifidobacteria (10^9/mL) in saline. EO + BI group, bifidobacteria (10^9/mL) in saline as the only vehicle for 42 days; EO + CPFX + saline group (EO + CP + Sal), CPFX for 6 days with started 48 h after *E. coli* inoculation, then normal saline for 42 days. EO + CPFX + bifidobacteria group (EO + CP + BI), CPFX for 6 days with started 48 h after *E. coli* inoculation, then bifidobacteria (10^9/mL) in saline as vehicle for 42 days.

2.3. Tissue collection and preparation

All mice were anesthetized with an intraperitoneal (i.p.) injection of chloral hydrate (400 mg/kg body weight) after the experimental period, and testes were removed bilaterally in the normal model (Sal, BI, CP, CP + Sal and CP + BI groups). Only right orchiectomy was performed in the epididymitis-orchitis model (Con, EO, EO + BI, EO + CP + Sal and EO + CP + BI groups) respectively. These removed testicles were transected into two halves. One half was fixed in 4% paraformaldehyde, while the remaining half was quickly frozen in liquid nitrogen and stored in −80 °C until further processing. The fixed samples were processed for embedding in paraffin wax. Serial sections were cut (6-μm thickness) and mounted on chrome alum gelatin-coated slides. They were then dewaxed, rehydrated and submitted to HE staining and immunohistochemical staining procedures. One part of each frozen sample was processed for total protein detection by Western blotting and Luminex multianalyte cytokine profiling (xMAP). Nuclear proteins were extracted from the frozen samples to detect NF-κB by Western blotting. Total RNA was isolated from the other part of the frozen testes, and quantification of mRNA was carried out by real-time PCR.

2.4. Testosterone measurements

Mice were anesthetized with an i.p. injection of chloral hydrate (400 mg/kg body weight) and immediately dissected to access the heart. Blood was collected and centrifuged at 1000 × *g* for 20 min at 4 °C to isolate the serum. If the serum was not used immediately, it was kept at −80 °C until further analysis. Serum testosterone concentrations from individual mice and the aliquot of supernatant from testicular homogenate were assayed by radioimmunoassays (RIA). The sensitivity and intra-assay and inter-assay coefficients of variation of the RIA were 13 pg/tube, 8.9% and 13.6%, respectively.

2.5. Cytokine measurements

The xMAP technology (Austin, TX, USA) was used to measure cytokine levels. Bead sets were coated with capture antibodies for various cytokines [TNF-α, IL-1β, transforming growth factor-α (TGF-α), interleukin-10 (IL-10)]. Fluorescence detection antibodies were then applied to bind the cytokine-capture antibody complex on the bead set. Multiple cytokines in the samples were then recognized by the differences in bead sets with fluoregenic emission detection using flow cytometric analysis. Each sample was measured in triplicate.

2.6. Biochemical analyses

An aliquot of the supernatants were tested in biochemical assays. The activities of total SOD was used as indices of antioxidant capacity.

Malondialdehyde (MDA) was used as reliable markers of lipid peroxidation. The level of SOD and MDA was detected by biochemical assays as last paper described (Zhao et al., 2013). These indices were determined according to the manufacturer's instructions of the assay kits (Jiancheng Bioengineering Institute, Nanjing, China). In brief, each testis tissue was incubated with 10 mM 2,4-dinitrophenylhydrazine in 2.5 M HCl at room temperature for 60 min. Subsequently, sample was precipitated with 20% (w/v) trichloroacetic acid, left on ice for 5 min and then centrifuged at $10{,}000 \times g$ for 10 min at 4 °C. The pellet was washed five times with 500 µL of a 1:1 (v/v) ethanol: ethyl acetate mixture. The final pellet was dissolved in 6 M guanidine hydrochloride. The absorbance was read at 370 nm spectrophotometrically, and the results were expressed as nmol carbonyls/mg protein.

2.7. Immunohistochemistry

The testicular sections of 6 um thick were stained with immunohistochemical staining was performed using routine procedures. Briefly, the sections were immersed in 3% hydrogen peroxide to block endogenous peroxidase and incubated for 5–10 min. After exposure in a moist chamber to goat serum (diluted 1:200, Santa Cruz Biotechnology, Santa Cruz, CA, USA) at 20 °C for 10 min, the unwashed sections were incubated overnight at 4 °C with anti-3β-HSD anti-sera (Santa Cruz Biotechnology, 1:100). The signal was detected by adding a biotinylated secondary antibody and streptavidin-peroxidase, followed by staining using 3,3′-diaminobenzidine plus peroxide solution. Sections were dehydrated using a series of graded alcohol (70%, 95%, 100%, absolute), cleared in xylene and cover-slipped with neutral gum. The numbers of positive stains Leydig cells in all slides were measured under microscope at 400 times high magnification. The number of positive Leydig cells of each specimen was obtained by calculating the average of 10 visual fields.

2.8. Real-time PCR and Western blotting

RNA was isolated from testis tissues by Trizol Reagent (Invitrogen, Carlsbad, CA, USA). Total RNA (2 mg) was reverse transcribed into cDNA by using the SuperScript First-Strand Synthesis System (Invitrogen). Quantification of mRNA was performed using real-time PCR according to the manufacturer's instructions for SYBR Premix Ex Taq using a real-time thermal cycler (Bio-Rad, Hercules, CA, USA). Results were expressed as optimal density ratios to *β-actin*. The primer sequences are listed in Table 1.

Animal tests were perfused with cold saline. Testes were isolated on ice and homogenized in lysis buffer, which was prepared by adding protease inhibitors (0.5% phenyl methylsulfonyl fluoride, 0.1% pepstatin, 0.1% leupeptin, 0.1% aprotinin) to TBS-T (20 mM Tris–HCl, pH7.6, 137 mM NaCl, 0.1% Tween-20). After centrifugation at $12{,}000 \times g$ for 20 min at 4 °C, the supernatant was collected, and the protein concentration was measured with the Pierce BCA protein assay kit (Thermo Scientific, Rockford, IL, USA). For NF-κB nuclear localization experiments, the nuclear fraction was extracted using a commercial kit following the manufacturer's protocol (Thermo Scientific, Pierce Protein Biology Products). Each protein sample (50 µg) was separated by sodium dodecyl sulfate polyacrylamide gel electrophoresis (SDS-PAGE) on a 10% gel (for Sirt1, DBC1, NF-κB, IL-1β, P450scc) or 12% gel (for steroidogenic acute regulatory protein, StAR) and then transferred to nitrocellulose membranes. The membranes were incubated in blocking buffer containing 5% fat-free milk in TBS-T for 2 h at room temperature and then incubated with antibodies against Sirt1 (1:1000 Abcam), DBC1 (1:1000 Abcam) NF-κB (Santa Cruz 1:1000), P450scc (Chemicon, Billerica, MA, USA, 1:1000), IL-1β (1:1000, Abcam) and StAR (Santa Cruz Biotechnology, 1:1000) overnight with constant agitation at 4 °C. After washing three times, the blots were incubated with corresponding horseradish peroxide-conjugated secondary antibodies (Amersham, Piscataway, NJ, USA, 1:5000) for 90 min at room temperature. Immunoreactive proteins were detected by using the enhanced chemiluminescence method (ECL kit, Amersham) and quantified by transmittance densitometry using volume integration with Gel-Pro software. To ensure even loading of the samples, the same membrane was probed with a rabbit anti-human β-actin antibody (Santa Cruz Biotechnology, 1:5000) or an anti-histone H3 antibody (Bioworld, Dublin, OH, USA, 1:1000).

Table 1
The primer sequence for real-time PCR.

Gene	Forward primer	Reverse primer
Sirt1	GTGTCATAGGCTAGGTGGTG	TGAAGAGGTGTTGGTGGC
NF-κB	CCAAAGAAGGACACGACAG	TGTGGATGGCATTTAGACC
actin	AGGCCCAGAGCAAGAGAGGTA	TCTCCATGTCGTCCCAGTG

Sirt1: Silent Mating Type Information Regulation 2 Homolog 1, NF-κB: nuclear factor kappa beta.

2.9. Data analysis

All data were analyzed using SPSS 21, and results are presented as the mean value ± SD. For all statistical analyses, a value of $P < 0.05$ was considered significant for $n = 10$, where n corresponds to the number of samples. Data were analyzed using one-way ANOVA with complete random design, followed by Student-Newman-Keuls *post hoc* tests for multiple pair-wise comparisons.

3. Results

3.1. Reversal of CPFX-induced variation in testicular weight, the seminiferous epithelium and the number of Leydig cells by probiotic microbes

CPFX administering caused a decrease in testicular weight in normal mice and infected mice (Fig. 1A, B, $P < 0.05$ compared to Con and EO groups). CP + BI and EO + CP + BI groups have a slight increased testicular weight compared to CPFX administering groups (Fig. 1A, B, $P < 0.05$). Histological findings in the examined groups by immunohistochemical staining are summarized in Fig. 1C, D. Immunohistochemical staining for 3β-HSD revealed positive cells in the interstitial tissue of the testes, and 3β-HSD protein was expressed in plasmid of Leydig cells. 3β-HSD protein is known as a marker of Leydig cells. The Con, Sal and BI groups revealed clustering Leydig cells and a regular seminiferous tubule morphology (Fig. 1C, D). In the CP group, seminiferous epithelium became irregular and Leydig cells stained by 3β-HSD decreased compared with Sal and BI (As shown by the arrow, Fig. 1C, E, $P < 0.01$). In the EO group, seminiferous epithelium damage: the wall of tube became irregular and thinner with spermatogenic cells lower, and Leydig cells stained by 3β-HSD showed no significant variation compared with Con groups (As shown by the arrow Fig. 1D, F, $P > 0.05$). In the EO + CP + Sal group, the number of Leydig cells showed a slight decrease compared to Con groups. (Fig. 1D, F, $P < 0.05$), and seminiferous epithelium showed no variation compared with the EO group. The probiotic microbes administering groups (CP + BI and EO + CP + BI) have a slight reversal in the seminiferous tubule morphology and Leydig cells (As shown by the arrow, Fig. 1C, D, E, F, $P < 0.05$). In the BI and EO + BI groups, the number of Leydig cells and seminiferous epithelium showed no variation compared with Con and EO groups ($P > 0.05$, Fig. 2C, D), which suggested that probiotics alone had no effect on the number of Leydig cells and seminiferous epithelium in normal and infected models.

The results showed that CPFX caused testicular histological damage and the number of Leydig cells decreased. Bifidobacteria effectively improved these damage to testicular structure and Leydig cells.

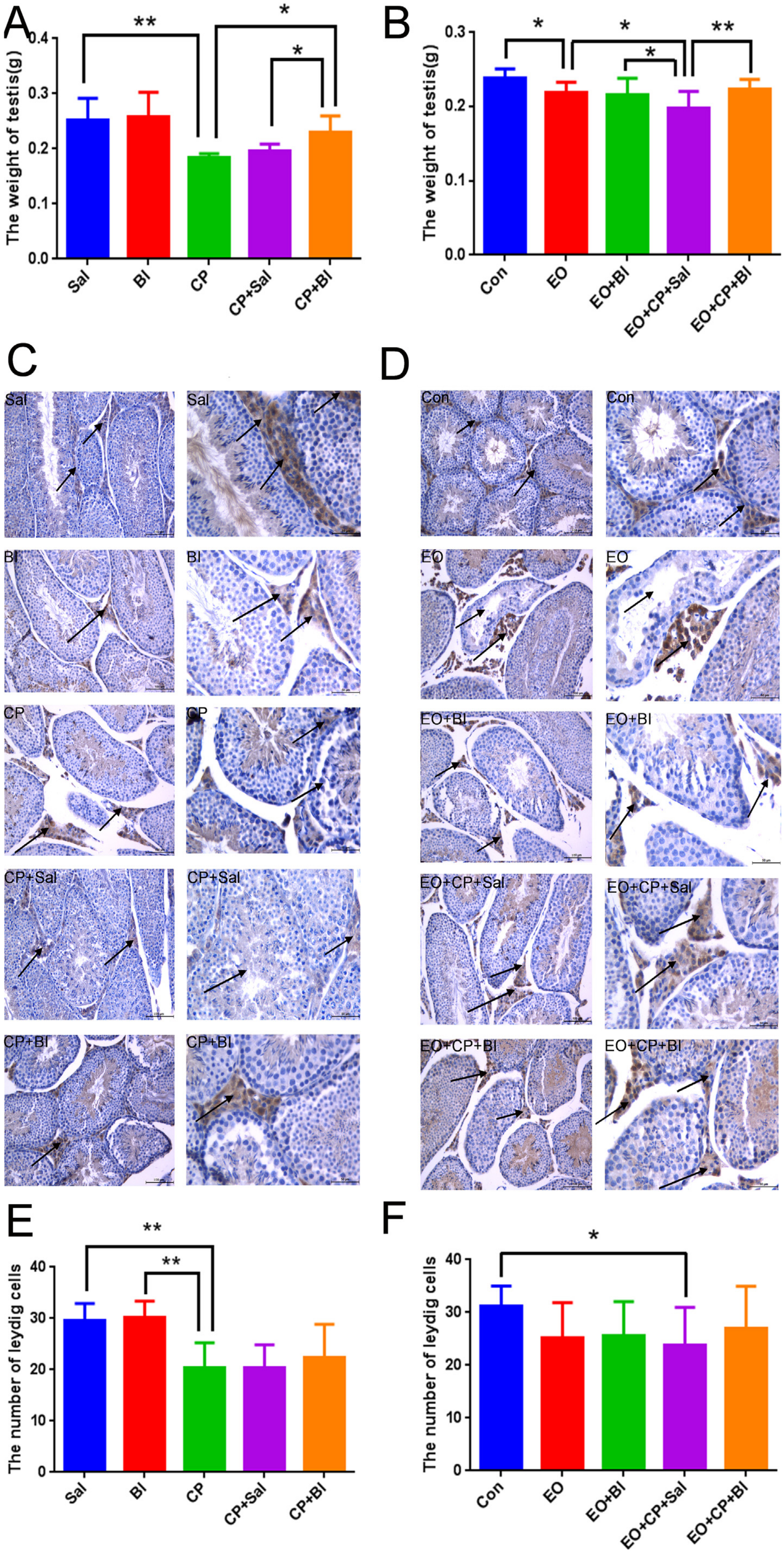

Fig. 1. Reversal of CPFX-induced variation in testicular weight, seminiferous epithelium and the number of Leydig cell by probiotic microbes. (A) The level of testicular weight in normal model. (B) The level of testicular weight in the infected model. (C) Testicular structure by 3β-HSD immunohistochemical staining in normal model. (D) Testicular structure by 3β-HSD immunohistochemical staining in infected model. (E) Leydig cell variables in numbers by 3β-HSD immunohistochemical staining in normal model. (F) Leydig cell variables in numbers by 3β-HSD immunohistochemical staining in the infected model. The arrow show the variation in seminiferous epithelium and the number of Leydig cell. Arrows indicate positive Leydig cells and spermatogenic tubules structure. $^{*}P < 0.05$, $^{**}P < 0.01$, $^{***}P < 0.001$.

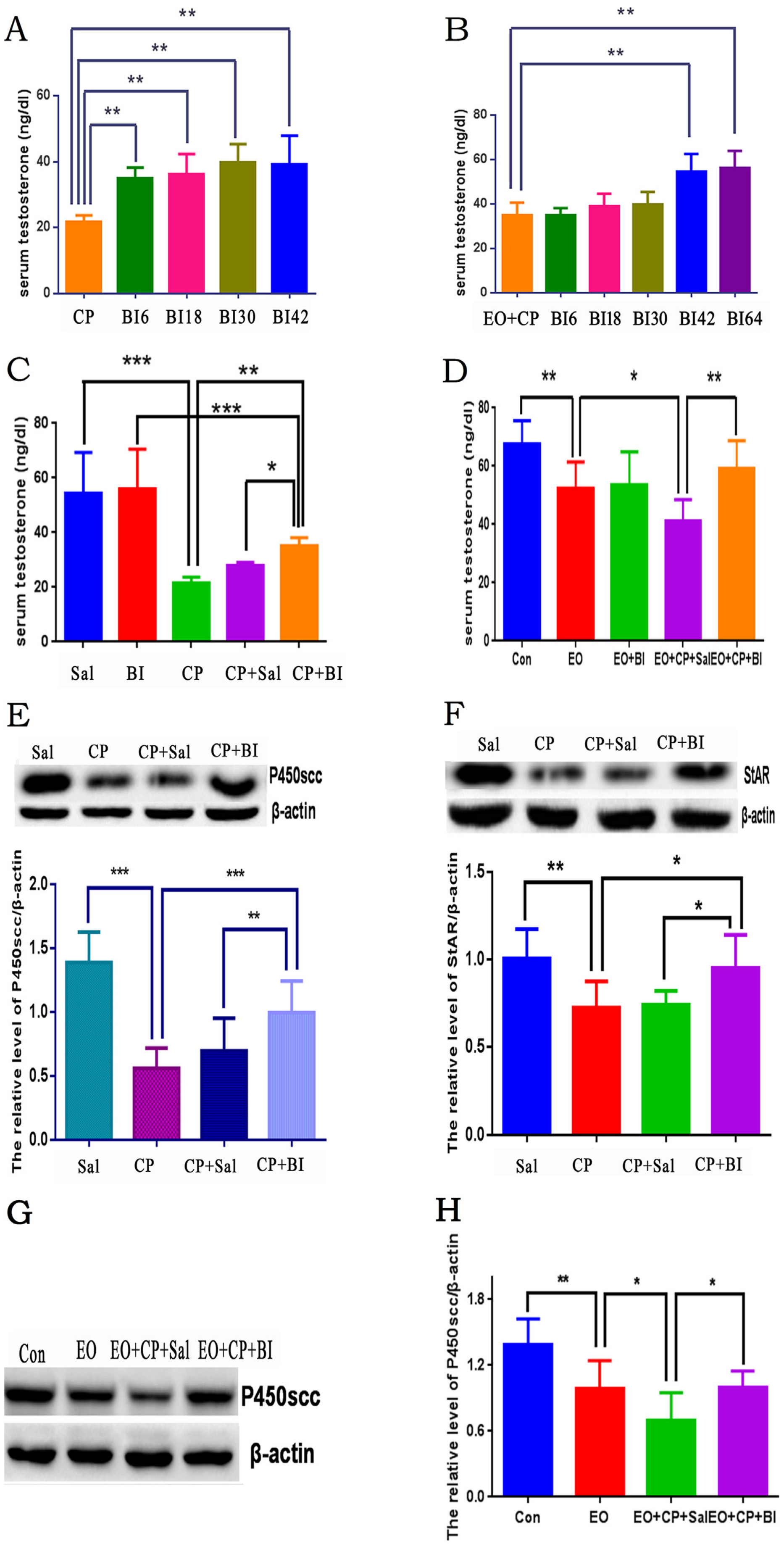

Fig. 2. Reversal of CPFX-induced reduction of testosterone levels and expression of steroidogenic enzymes by probiotic microbes. (A, B) Testosterone level is in a time-dependent manner in normal model and infected model. (C) Levels of serum testosterone in normal model. (D) Levels of serum testosterone in the infected model. (E, F) Testis extracts were analyzed by Western blotting using anti-P450scc, anti-StAR and anti-β-actin antibodies in normal model. Relative band intensities of P450scc and StAR are expressed as ratios to β-actin. Data are means ± SD (n = 6) for the Sal, CP, CP + Sal and CP + BI groups. (G, H) Testis extracts were analyzed by Western blotting using anti-P450scc, anti-β-actin antibodies in infected model. Relative band intensities of P450scc are expressed as ratios to β-actin. Data are means ± SD (n = 6) for the con, EO, EO + CP + Sal and EO + CP + BI groups. $^{*}P < 0.05$, $^{**}P < 0.01$, $^{***}P < 0.001$.

3.2. Reversal of CPFX-induced reduction of testosterone levels and expression of steroidogenic enzymes by probiotic microbes

The level of serum testosterone and expression of steroidogenic enzymes in the normal model and infected model are shown in Fig. 2. These animals in CP group were administered with 1×10^9 cfu/ml bifidobacteria for the different time periods (from 6 to 64 days) in different model. As shown in Fig. 2A, B, testosterone level is in a time-dependent manner. In normal model, results of the RIA assay showed that testosterone level was increased significantly in CP + BI group than CP group, so bifidobacteria (10^9/mL) as vehicle for 6 days is valid time. In epididymitis-orchitis model, the results showed that testosterone level was increased significantly in BI_{42} and BI_{64} than other groups, so bifidobacteria (10^9/mL) as vehicle for 42 days is valid time.

Serum testosterone levels (Fig. 2C) were significantly increased in the CP + BI group compared with the CP ($P < 0.01$) and CP + Sal groups ($P < 0.05$), while they were lower in the CP group compared with the Sal and BI group ($P < 0.01$). Serum testosterone levels (Fig. 2D) were significantly increased in EO + CP + BI than EO + CP + Sal group ($P < 0.01$). Serum testosterone (Fig. 2D) levels in the EO + CP + Sal group were lower than that of EO group ($P < 0.05$). In the BI and EO + BI groups, serum testosterone levels had no significantly variation compared with corresponding Con and EO groups ($P > 0.05$, Fig. 2C, D), which suggested that probiotics alone had no effect on serum testosterone in the normal and infected models.

Meanwhile, P450scc levels (Fig. 2E) were significantly higher in the CP + BI group compared with the CP ($P < 0.001$) and CP + Sal groups ($P < 0.01$), and they were lower in the CP group compared with the Sal group $P < 0.001$). StAR (Fig. 2F) levels were also significantly increased in the CP + BI group compared with the CP ($P < 0.05$) and CP + Sal groups ($P < 0.05$), while they were decreased in the CP group compared with the Sal group ($P < 0.01$).

Meanwhile, P450scc levels (Fig. 2G, H) were also significantly higher in EO + CP + BI than EO + CP + Sal group ($P < 0.05$), EO + CP + Sal group were lower than EO group ($P < 0.05$).

The results showed that these animals received bifidobacteria were statistically increase in level of testosterone and steroidogenic enzymes than those of animals which received CPFX. These results indicated that administration of bifidobacteria effectively elevated testosterone, steroidogenic enzymes levels after CPFX administration.

3.3. Reversal of CPFX-induced reduction of Sirt1 expression by probiotic microbes

We detected Sirt1 expression by Western blotting (Fig. 3A) and real-time PCR in the normal model (Fig. 3B). These analyses showed consistently that the levels of Sirt1 were significantly higher in the CP + BI group compared with the CP ($P < 0.001$) and CP + Sal groups ($P < 0.01$), while they were lower in the CP group compared with the Sal group ($P < 0.001$).

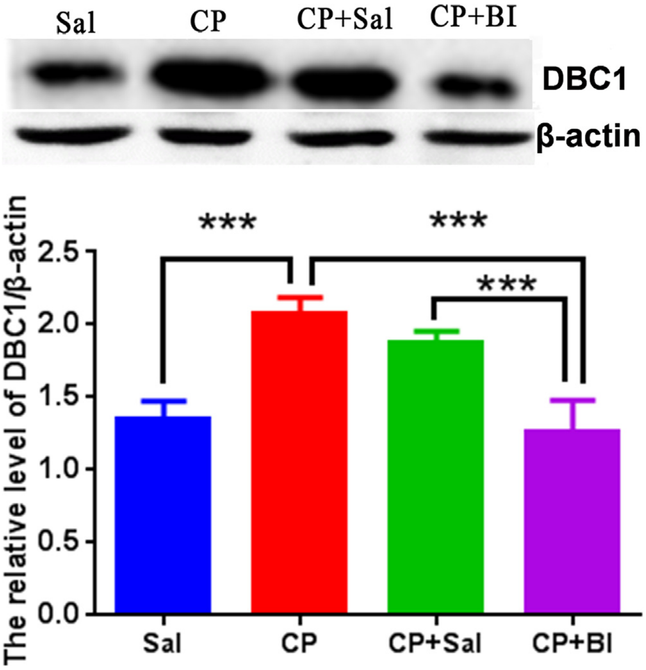

Fig. 4. Reversal of CPFX-induced reduction of DBC1 expression by probiotic microbes. DBC1 expression was detected in normal model by Western blotting. Relative DBC1 band intensities are shown as ratios to β-actin. *P < 0.05, **P < 0.01, ***P < 0.001.

We also detected Sirt1 expression by western blotting in the infected model (Fig. 3C). Sirt1 levels were increased in the EO + CP + BI group than that of EO ($P < 0.05$) and EO + CP + Sal group ($P < 0.001$). EO + CP + Sal group were significantly lower than EO group ($P < 0.05$).

These results showed that administration of bifidobacteria resulted in effective elevation of Sirt1 levels after CPFX administration.

3.4. Reversal of CPFX-induced reduction of DBC1 expression by probiotic microbes

Western blotting was used to assess the effect of probiotic microbes on reversing CPFX-induced DBC1 expression in testis samples (Fig. 4). The results showed that the level of DBC1 was significantly lower in the

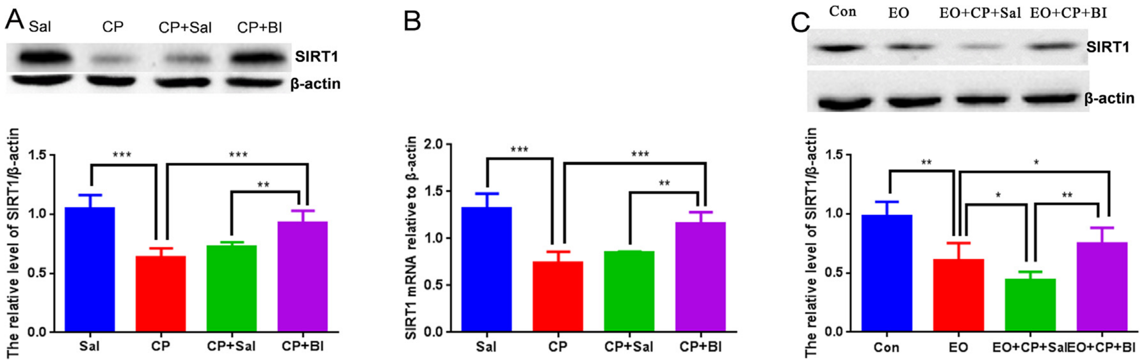

Fig. 3. Reversal of CPFX-induced reduction of Sirt1 expression by probiotic microbes. (A) Detection of Sirt1 expression in normal model by Western blotting. Relative Sirt1 band intensities are shown as ratios to β-actin. (B) Detection of Sirt1 expression in normal model by real-time PCR. Values are means ± SD (n = 6). (C) Detection of Sirt1 expression in the infected model by Western blotting. Relative Sirt1 band intensities are shown as ratios to β-actin.*P < 0.05, **P < 0.01, ***P < 0.001.

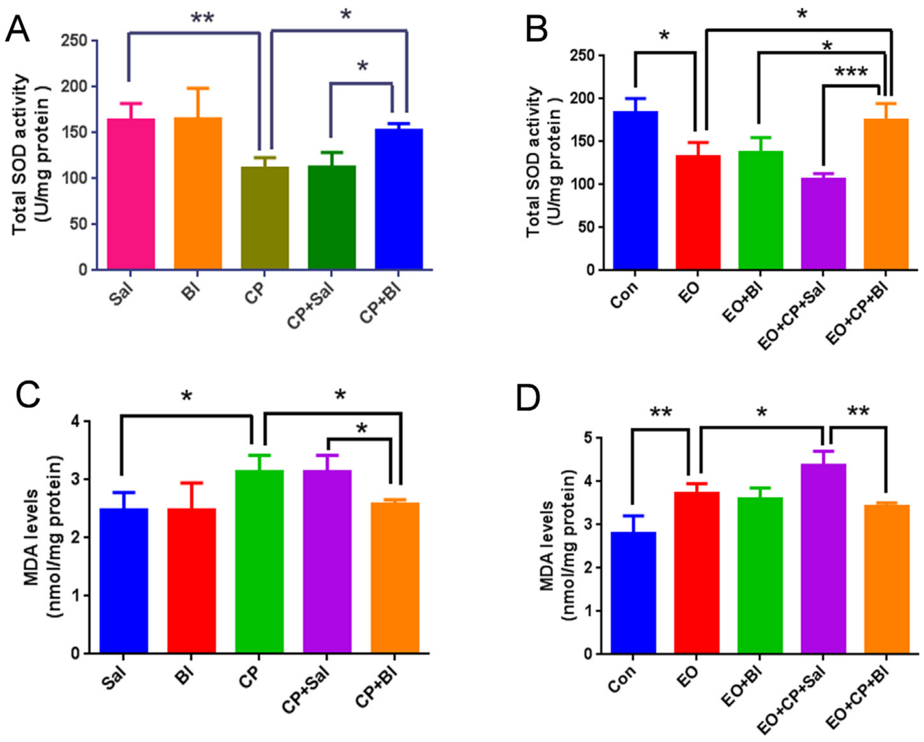

Fig. 5. Reversal of CPFX-induced oxidative stress by probiotic microbes. (A) The total SOD activity was detected in the normal model by biochemical assays. (B) The total SOD activity was detected in the infected model by biochemical assays. (C) The level of MAD was detected in the normal model by biochemical assays. (D) The level of MAD was detected in the infected model by biochemical assays. Values are means ± SD (n = 6). $^{*}P < 0.05$, $^{**}P < 0.01$, $^{***}P < 0.001$.

CP + BI group compared with the CP ($P < 0.001$) and CP + Sal ($P < 0.001$) groups, while it was higher in the CP group compared with the Sal ($P < 0.001$) group. These results showed that administration of bifidobacteria after CPFX resulted in a more effective decrease of the DBC1 level.

3.5. Reversal of CPFX-induced oxidative stress by probiotic microbes

We detected oxidative damage (MDA) and anti-oxidative enzymes (SOD) by biochemical assays in the normal and infected model. The result showed that the level of SOD were significantly increased in the CP + BI group compared with the CP and CP + Sal groups (Fig. 5A, $P < 0.05$), and the level of MDA was significantly decreased in the CP + BI group compared with the CP and CP + Sal groups (Fig. 5C, $P < 0.05$). The same result showed that SOD in the EO + CP + BI group were significantly increased than EO + CP + Sal group (Fig. 5B $P < 0.05$), and MDA were decreased in the EO + CP + BI group compared with EO + CP + Sal groups (Fig. 5D $P < 0.05$). These results showed that administration of bifidobacteria after CPFX could attenuate oxidative damage and significantly elevate anti-oxidative enzymes.

3.6. Reversal of CPFX-induced NF-κB nuclear translocation by probiotic microbes

We detected NF-κB transcription factor by western blotting analysis of nuclear protein extracts of testes (Fig. 6A) and real-time PCR in the normal model (Fig. 6B) These analyses showed consistently that the level of NF-κB was significantly decreased in the CP + BI group compared with the CP ($P < 0.01$) and CP + Sal groups ($P < 0.05$), and it was increased in the CP group compared with the Sal group ($P < 0.001$).

We also detected NF-κB transcription factor by western blotting analysis of nuclear protein extracts of testes in the infected model (Fig. 6C). NF-κB levels in the EO + CP + BI group were significantly decreased than EO + CP + Sal group ($P < 0.05$). NF-κB levels were decreased in the EO + CP + Sal group compared with EO groups ($P < 0.05$).

These results showed that the level of NF-κB in nuclear increased in the normal testicles of animals which received CPFX, but the level of NF-κB in nuclear decreased in the infected testicles of animals which received CPFX. Eventually, administration of bifidobacteria after CPFX contributed to attenuated NF-κB protein levels in normal and infected model.

3.7. Reversal of CPFX-induced increase of testicular inflammatory cytokines and decrease of anti-inflammatory cytokines levels by probiotic microbes

The levels of IL-1β, TNF-α, IL-10 and TGF-α were measured in the testes by using xMAP technology in normal model (Fig. 7E, F, G, H). We also detected IL-1β expression by Western blotting in normal and infected model (Fig. 7A, B, C, D). IL-1β protein (Fig. 7A, C) were significantly decreased in the CP + BI group compared with the CP and CP + Sal groups ($P < 0.05$), while they were increased in the CP group compared with the Sal group ($P < 0.001$). IL-1β protein (Fig. 7B, D) in the EO + CP + BI group were significantly decreased than EO + CP + Sal group ($P < 0.05$). IL-1β protein were decreased in the EO + CP + Sal group compared with EO groups ($P < 0.05$).

Levels of IL-1β and TNF-α were significantly decreased in the CP + BI group compared with the CP and CP + Sal groups (Fig. 7E, F, $P < 0.05$), while they were increased in the CP group compared with the Sal group ($P < 0.001$). IL-10 and TGF-α levels were significantly increased in the CP + BI group compared with the CP and CP + Sal groups (Fig. 7G, H, $P < 0.05$), while they were decreased in the CP group compared with the Sal group ($P < 0.001$). These results showed that administration of bifidobacteria after CPFX could attenuate inflammatory cytokines and significantly elevate anti-inflammatory cytokines.

4. Discussion

In this study, we used normal model and infected model to isolate testicles and serum to assess the reversal of CPFX-induced variation in testicular weight, the number of Leydig cells, testosterone and steroidogenic enzymes by probiotic microbes. Our results consistent with

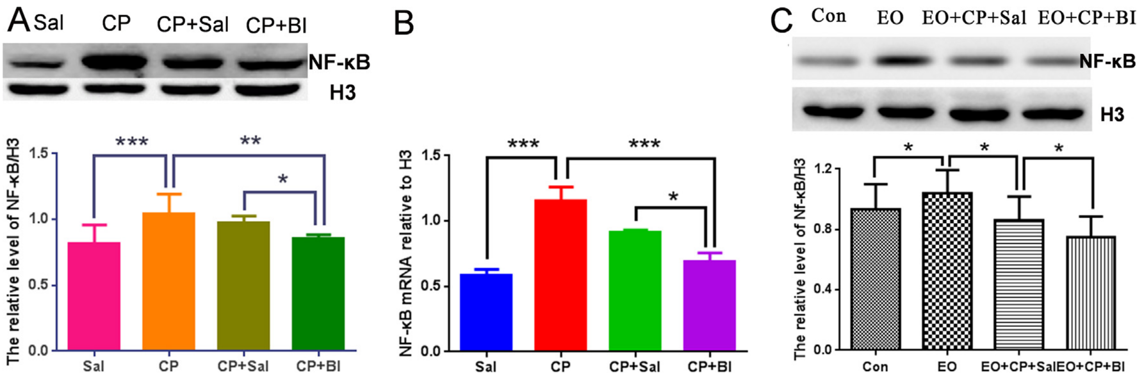

Fig. 6. Reversal of CPFX-induced NF-κB nuclear translocation by probiotic microbes. (A) Testis nuclear extracts were analyzed in normal model by Western blotting using an anti-NF-κB antibody. Relative NF-κB band intensities are shown as ratios to H3. (B) Detection of NF-κB expression by real-time PCR. Values are means ± SD (n = 6). (C) Testis nuclear extracts were analyzed in the infected model by Western blotting using an anti-NF-κB antibody. Relative NF-κB band intensities are shown as ratios to H3. $^{*}P < 0.05$, $^{**}P < 0.01$, $^{***}P < 0.001$.

those reported in the literature (Demir et al., 2007) showed that CPFX treatment resulted in a marked testicular atrophy and reduction in the number of Leydig cells. Probiotic microbes can reverse the variation in testicular atrophy and the number of Leydig cell of these mice, and enhance the levels of circulating testosterone and steroidogenic enzymes compared to their controls which received CPFX treatment. The results suggested a gonadotoxic potential for CPFX, which is the first time to show the reversal effect of probiotics on CPFX's damage to testicles. Probiotics that exert benefit in sufficient amounts are considered as a promising tool for reduction the risk of antibiotics associated diarrhea (AAD), and meantime rebalance the gut microbiota (GM) (Hempel et al., 2012), prevention age-related testicular atrophy and male hypogonadism without the controversy and side-effect risks of testosterone replacement therapy (Zobeiri et al., 2013). Our findings are consistent with these studies of probiotics. However, the underlying mechanism responsible for the reversal effect of probiotics on CPFX-induced damage in Leydig cells is still to be determined. Similar testicular health benefits were produced using systemic depletion of the oxidative damage and pro-inflammatory cytokine, implicating a chronic oxidative stress and inflammatory state in the reduction of testosterone. Based on these observations, we propose a model whereby probiotic bacteria modulate gastrointestinal microbiota resulting in systemic effects on redox state and the immune system that activate metabolic pathways that restore tissue homeostasis and overall health.

We investigated the recovery effect of probiotics on biomarkers of oxidative stress and inflammation state due to ciprofloxacin-induced reduction of testosterone in male mice. In the present study, ciprofloxacin treatment produced high levels of oxidative damage, as evidenced by a significant elevation in MDA and a significant decrease in SOD content. Lipid peroxidation is a significant determinant of the degree of oxidative damage with MDA being one of the products as well as an important marker of the process of the oxidative stress (Valenzuela, 1991). Previous studies have reported fluoroquinolone-induced increase in tissue MDA level and decrease in GSH content (Pouzaud et al., 2006; Altinordulu and Eraslan, 2009). However, probiotics induced a significant decrease in the MDA, efficiently improved the ciprofloxacin-induced suppression of SOD activities and Sirt1 in our study. These results are in consistence with previous reports that administration of probiotics (300 g/day) for 6 weeks results in significant increase in the activity of both erythrocyte SOD and GPx in type 2 diabetes mellitus (T2DM) patients (Ejtahed et al., 2012). As expected, ciprofloxacin treatment resulted in significant testosterone reduction in mice, and probiotics possessed protective effects on the ciprofloxacin-induced testicular damage and testosterone reduction by inhibiting oxidative stress.

Our findings showed that probiotics has significant effect in prevention of ciprofloxacin-induced inflammatory state in testis tissue. The results exhibited a significant increase in serum level of TNF-a, IL-1β, NF-κB and accompanied by Sirt1 and anti-inflammatory cytokines decreased. Sirt1, a member of the silent information regulator (Sir2) family, belongs to class III histone/protein deacetylases (HDACs) (Dai et al., 2016). Sirt1 has been suggested to be involved in various cellular processes, including gene silencing, glucose and lipid metabolism, stress resistance and extension of life span in response to caloric restriction (Xu et al., 2018; Ji et al., 2018; Liang et al., 2018). Sirt1 protein is much more abundant in male testis, compared with other tissues, including liver, skeletal and muscle tissues. DBC1 is a key physiological regulator of Sirt1 activity, and the activation of Sirt1 during fasting previously was described to be mediated by the dissociation of the Sirt1-DBC1 complex (Li et al., 2019). The regulation of Sirt1 by DBC1 may influence energy metabolism, aging and cancer cell biology, as well as exert anti-inflammatory effects and protect from inflammatory stress. Interestingly, the activity of SIRT1 was controlled by oxidative stress and the increased levels of ROS. The balance between Sirt1 and ROS governs inflammatory responses, oxidative state and autophagy (Salminen et al., 2013). The present study showed that probiotics can significantly inhibit the escalation of oxidative stress following ciprofloxacin administration, and up-regulate Sirt1. SIRT1 can inhibit NF-κB signaling that is a major inducer of inflammatory responses (Bai et al., 2018) and also been reported to stimulate the expression of antioxidants to resist oxidative stress (Yang et al., 2016). Sirt1 acted anti-inflammatory effects by the deacetylation of NF-kB, which is a central component of the intracellular inflammatory response (Magni et al., 2018). Pro-inflammatory cytokines, such as TNF-α and IL-1β, have been proved to inhibit testicular Leydig cell steroidogenesis at the level of expression of steroidogenic enzymes (Leisegang and Henkel, 2018; Bornstein et al., 2004; Tremellen et al., 2018). Probiotics can significantly inhibit the level of pro-inflammatory cytokines TNF-a and IL-1β, and increase anti-inflammatory cytokines IL-10 and TGF-α in our study. Several studies in humans and mice have investigated probiotics to treat infectious disease and boost the immune system during antibiotic therapy (Mestre et al., 2018; Lazar et al., 2018; Grandiosa et al., 2018). The results of our study showed that the testis-protective, antiinflammatory and antioxidation effects of probiotics largely resulted from its ability to decrease oxidative stress and preserve antioxidant activity by stabilizing antioxidant defense systems, reducing Lipid peroxidation and decreasing pro-inflammatory factors. Therefore, in view of the critical role of these above mediators in reducting testosterone, probiotics could inhibit ciprofloxacin induced testis damage via amelioration of oxidative stress and inflammatory response.

Declaration of Competing Interest

The authors declare that they have no known competing financial

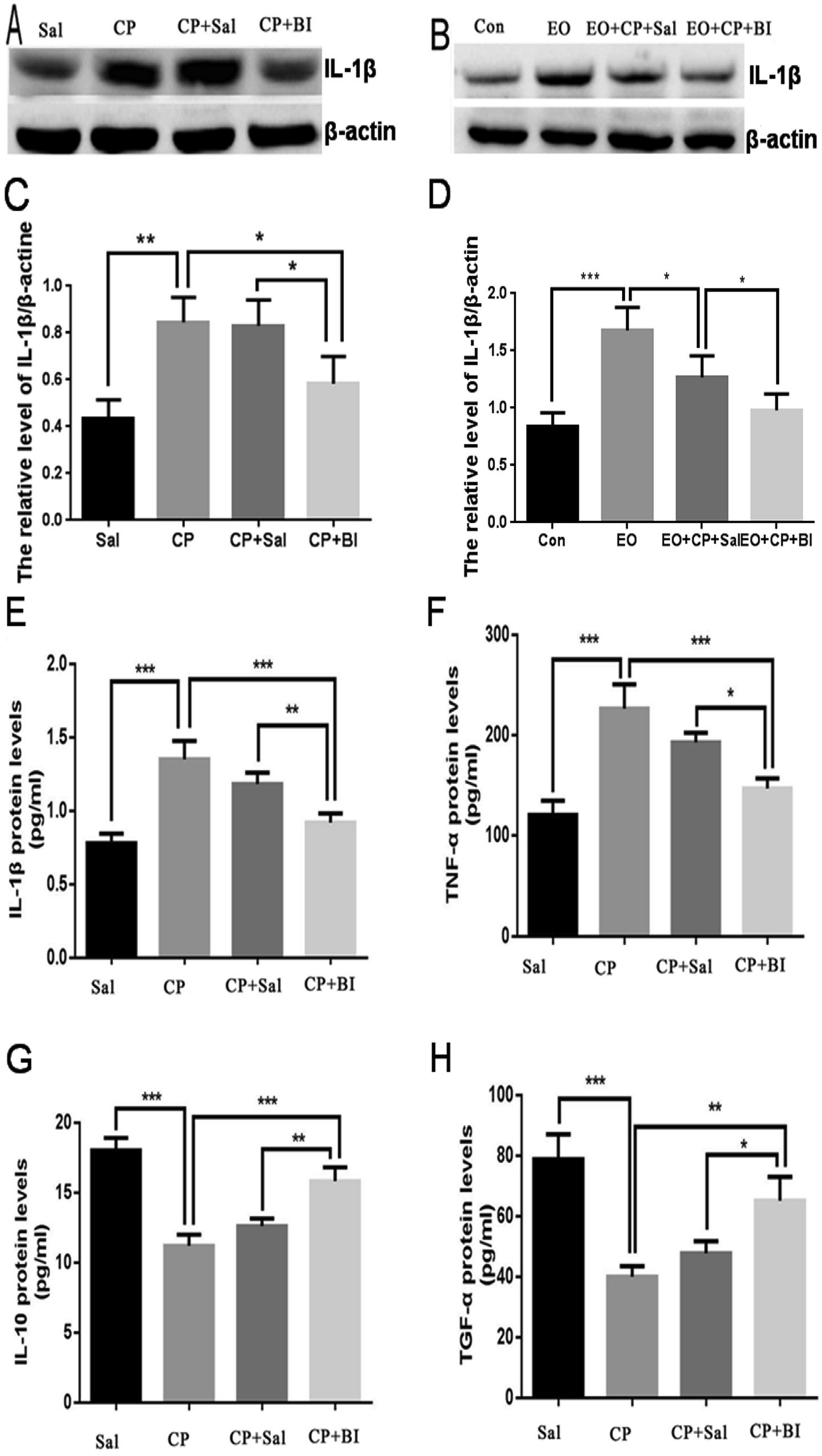

Fig. 7. Reversal of CPFX-induced increase of testicular inflammatory cytokines and decrease of anti-inflammatory cytokine levels by probiotic microbes. (A, C) Detection of IL-1β expression in normal model by Western blotting. Relative IL-1β band intensities are shown as ratios to β-actin. (B, D) Detection of IL-1β expression in the infected model by Western blotting. Relative IL-1β band intensities are shown as ratios to β-actin. (E, F) Levels of inflammatory cytokines in normal group by xMAP technology. (G, H) Levels of anti-inflammatory cytokines in normal group by xMAP technology. Values are means ± SD (n = 6). *P < 0.05, **P < 0.01, ***P < 0.001.

interests or personal relationships that could have appeared to influence the work reported in this paper.

Acknowledgments

The authors thank National Key Research and Development Program (Grant no. 2016YFF0202300, awarded to P. Lv) and Natural Science Foundation of Hebei Province, China (Grant no. H2019206212, awarded to P. Lv), Hebei high-level personnel funding project (A201905006, awarded to P. Lv) for supporting this research. We also thank Yanqing Bian and Yanzhong Chang for the efforts and facilities in the whole experiment.

Author contributions

Authors' contribution to the work described in the paper: Congcong Xie,Yanqing Bian, Helin Feng, Yaru Li, Dong Zhang, Yangyang Tian, Yu Zhao performed research. Lixuan Wang, Li Li, ShiYang Chang analyzed the data. Hang Li, Xiujun Zhao, Pin Lv designed the research study and wrote the paper. All authors have read and approved the final version of the manuscript.

References

Altinordulu, S., Eraslan, G., 2009. Effects of some quinolone antibiotics on malondialdehyde levels and catalase activity in chicks. Food Chem. Toxicol. 47, 2821–2823.

Asemi, Z., Zare, Z., Shakeri, H., Sabihi, S.S., Esmaillzadeh, A., 2013. Effect of multispecies probiotic supplements on metabolic profiles, hs-CRP, and oxidative stress in patients with type 2 diabetes. Ann. Nutr. Metab. 63, 1–9.

Bai, X.Z., Zhang, J.L., Liu, Y., Zhang, W., Li, X.Q., Wang, K.J., Cao, M.Y., Zhang, J.N., Han, F., Shi, J.H., Hu, D.H., 2018. MicroRNA-138 aggravates inflammatory responses of macrophages by targeting SIRT1 and regulating the NF-kappaB and AKT pathways. Cell. Physiol. Biochem. 49, 489–500.

Bornstein, S.R., Rutkowski, H., Vrezas, I., 2004. Cytokines and steroidogenesis. Mol. Cell. Endocrinol. 215, 135–141.

Bubnov, R.V., Babenko, L.P., Lazarenko, L.M., Mokrozub, V.V., Spivak, M.Y., 2018. Specific properties of probiotic strains: relevance and benefits for the host. EPMA J. 9, 205–223.

Dai, W., Zhou, J., Jin, B., Pan, J., 2016. Class III-specific HDAC inhibitor Tenovin-6 induces apoptosis, suppresses migration and eliminates cancer stem cells in uveal melanoma. Sci. Rep. 6, 22622.

Demir, A., Turker, P., Onol, F.F., Sirvanci, S., Findik, A., Tarcan, T., 2007. Effect of experimentally induced Escherichia coli epididymo-orchitis and ciprofloxacin treatment on rat spermatogenesis. Int. J. Urol. 14, 268–272.

Ejtahed, H.S., Mohtadi-Nia, J., Homayouni-Rad, A., Niafar, M., Asghari-Jafarabadi, M., Mofid, V., 2012. Probiotic yogurt improves antioxidant status in type 2 diabetic patients. Nutrition 28, 539–543.

Ermolenko, E., Rybalchenko, O., Borshev, Y., Tarasova, E., Kramskaya, T., Leontieva, G., Kotyleva, M., Orlova, O., Abdurasulova, I., Suvorov, A., 2018. Influence of monostrain and multistrain probiotics on immunity, intestinal ultrastructure and microbiota in experimental dysbiosis. Benef. Microbes 1–14.

Grandiosa, R., Merien, F., Young, T., Van Nguyen, T., Gutierrez, N., Kitundu, E., Alfaro, A.C., 2018. Multi-strain probiotics enhance immune responsiveness and alters metabolic profiles in the New Zealand black-footed abalone (Haliotis iris). Fish Shellfish Immunol. 82, 330–338.

Hempel, S., Newberry, S.J., Maher, A.R., Wang, Z., Miles, J.N., Shanman, R., Johnsen, B., Shekelle, P.G., 2012. Probiotics for the prevention and treatment of antibiotic-associated diarrhea: a systematic review and meta-analysis. JAMA 307, 1959–1969.

Holowacz, S., Guinobert, I., Guilbot, A., Hidalgo, S., Bisson, J.F., 2018. A mixture of five bacterial strains attenuates skin inflammation in mice. Antiinflamm. Antiallergy Agents Med. Chem. 17, 125–137.

Iskender, H., Yenice, G., Dokumacioglu, E., Hayirli, A., Sevim, C., Dokumacioglu, A., Terim Kapakin, K.A., 2018. Astaxanthin alleviates renal damage of rats on high fructose diet through modulating NFkappaB/SIRT1 pathway and mitigating oxidative stress. Arch. Physiol. Biochem. 1–5.

Ji, K., Sun, X., Liu, Y., Du, L., Wang, Y., He, N., Wang, J., Xu, C., Liu, Q., 2018. Regulation of apoptosis and radiation sensitization in lung cancer cells via the Sirt1/NF-kappaB/Smac pathway. Cell. Physiol. Biochem. 48, 304–316.

Kalghatgi, S., Spina, C.S., Costello, J.C., Liesa, M., Morones-Ramirez, J.R., Slomovic, S., Molina, A., Shirihai, O.S., Collins, J.J., 2013. Bactericidal antibiotics induce mitochondrial dysfunction and oxidative damage in mammalian cells. Sci. Transl. Med. 5, 192ra185.

Karamali, M., Eghbalpour, S., Rajabi, S., Jamilian, M., Bahmani, F., Tajabadi-Ebrahimi, M., Keneshlou, F., Mirhashemi, S.M., Chamani, M., Hashem Gelougerdi, S., Asemi, Z., 2018. Effects of probiotic supplementation on hormonal profiles, biomarkers of inflammation and oxidative stress in women with polycystic ovary syndrome: a randomized, double-blind, placebo-controlled trial. Arch. Iran. Med. 21, 1–7.

Lazar, V., Ditu, L.M., Pircalabioru, G.G., Gheorghe, I., Curutiu, C., Holban, A.M., Picu, A., Petcu, L., Chifiriuc, M.C., 2018. Aspects of gut microbiota and immune system interactions in infectious diseases, immunopathology, and cancer. Front. Immunol. 9, 1830.

Leisegang, K., Henkel, R., 2018. The in vitro modulation of steroidogenesis by inflammatory cytokines and insulin in TM3 Leydig cells. Reprod. Biol. Endocrinol. 16, 26.

Li, H., Tian, Z., Qu, Y., Yang, Q., Guan, H., Shi, B., Ji, M., Hou, P., 2019. SIRT7 promotes thyroid tumorigenesis through phosphorylation and activation of Akt and p70S6K1 via DBC1/SIRT1 axis. Oncogene 38 (3), 345–359. https://doi.org/10.1038/s41388-018-0434-6.

Liang, Q.X., Lin, Y.H., Zhang, C.H., Sun, H.M., Zhou, L., Schatten, H., Sun, Q.Y., Qian, W.P., 2018. Resveratrol increases resistance of mouse oocytes to postovulatory aging in vivo. Aging (Albany NY) 10, 1586–1596.

Liu, X., Ehmed, E., Li, B., Dou, J., Qiao, X., Jiang, W., Yang, X., Qiao, S., Wu, Y., 2016. Breast cancer metastasis suppressor 1 modulates SIRT1-dependent p53 deacetylation through interacting with DBC1. Am. J. Cancer Res. 6, 1441–1449.

Ludwig, M., Johannes, S., Bergmann, M., Failing, K., Schiefer, H.G., Weidner, W., 2002. Experimental Escherichia coli epididymitis in rats: a model to assess the outcome of antibiotic treatment. BJU Int. 90, 933–938.

Magni, M., Buscemi, G., Zannini, L., 2018. Cell cycle and apoptosis regulator 2 at the interface between DNA damage response and cell physiology. Mutat. Res. 776, 1–9.

Mestre, L., Carrillo-Salinas, F.J., Mecha, M., Feliu, A., Guaza, C., 2018. Gut microbiota, cannabinoid system and neuroimmune interactions: new perspectives in multiple sclerosis. Biochem. Pharmacol. 157, 51–66.

Nohr, M.K., Bobba, N., Richelsen, B., Lund, S., Pedersen, S.B., 2017. Inflammation downregulates UCP1 expression in brown adipocytes potentially via SIRT1 and DBC1 interaction. Int. J. Mol. Sci. 18.

Poutahidis, T., Springer, A., Levkovich, T., Qi, P., Varian, B.J., Lakritz, J.R., Ibrahim, Y.M., Chatzigiagkos, A., Alm, E.J., Erdman, S.E., 2014. Probiotic microbes sustain youthful serum testosterone levels and testicular size in aging mice. PLoS ONE 9, e84877.

Pouzaud, F., Dutot, M., Martin, C., Debray, M., Warnet, J.M., Rat, P., 2006. Age-dependent effects on redox status, oxidative stress, mitochondrial activity and toxicity induced by fluoroquinolones on primary cultures of rabbit tendon cells. Comp. Biochem. Physiol. C: Toxicol. Pharmacol. 143, 232–241.

Ryan, L., Daly, P., Cullen, I., Doyle, M., 2018. Epididymo-orchitis caused by enteric organisms in men > 35 years old: beyond fluoroquinolones. Eur. J. Clin. Microbiol. Infect. Dis. 37, 1001–1008.

Salminen, A., Kaarniranta, K., Kauppinen, A., 2013. Crosstalk between oxidative stress and SIRT1: impact on the aging process. Int. J. Mol. Sci. 14, 3834–3859.

Savignac, H.M., Tramullas, M., Kiely, B., Dinan, T.G., Cryan, J.F., 2015. Bifidobacteria modulate cognitive processes in an anxious mouse strain. Behav. Brain Res. 287, 59–72.

Shaki, F., Ashari, S., Ahangar, N., 2016. Melatonin can attenuate ciprofloxacin induced nephrotoxicity: involvement of nitric oxide and TNF-alpha. Biomed. Pharmacother. 84, 1172–1178.

Shen, Q., Shang, N., Li, P., 2011. In vitro and in vivo antioxidant activity of Bifidobacterium animalis 01 isolated from centenarians. Curr. Microbiol. 62, 1097–1103.

Singh, P., Hanson, P.S., Morris, C.M., 2017. SIRT1 ameliorates oxidative stress induced neural cell death and is down-regulated in Parkinson's disease. BMC Neurosci. 18, 46.

Steiner, A., Harapas, C.R., Masters, S.L., Davidson, S., 2018. An update on autoinflammatory diseases: relopathies. Curr. Rheumatol. Rep. 20, 39.

Tremellen, K., McPhee, N., Pearce, K., Benson, S., Schedlowski, M., Engler, H., 2018. Endotoxin-initiated inflammation reduces testosterone production in men of reproductive age. Am. J. Physiol. Endocrinol. Metab. 314, E206–E213.

Valenzuela, A., 1991. The biological significance of malondialdehyde determination in the assessment of tissue oxidative stress. Life Sci. 48, 301–309.

Wang, Y., Wu, Y., Xu, H., Mei, X., Yu, D., Li, W., 2017. Antioxidant properties of probiotic bacteria. Nutrients 9.

Xu, J., Li, Y., Lou, M., Xia, W., Liu, Q., Xie, G., Liu, L., Liu, B., Yang, J., Qin, M., 2018. Baicalin regulates SirT1/STAT3 pathway and restrains excessive hepatic glucose production. Pharmacol. Res. 136, 62–73.

Yang, D., Tan, X., Lv, Z., Liu, B., Baiyun, R., Lu, J., Zhang, Z., 2016. Regulation of Sirt1/Nrf2/TNF-alpha signaling pathway by luteolin is critical to attenuate acute mercuric chloride exposure induced hepatotoxicity. Sci. Rep. 6, 37157.

Zhao, X., Bian, Y., Sun, Y., Li, L., Wang, L., Zhao, C., Shen, Y., Song, Q., Qu, Y., Niu, S., Wu, W., Gao, F., 2013. Effects of moderate exercise over different phases on age-related physiological dysfunction in testes of SAMP8 mice. Exp. Gerontol. 48, 869–880.

Zobeiri, F., Sadrkhanlou, R.A., Salami, S., Mardani, K., 2013. Long-term effect of ciprofloxacin on testicular tissue: evidence for biochemical and histochemical changes. Int. J. Fertil. Steril. 6, 294–303.